International Journal of Bioelectromagnetism *www.ijbem.org*
Vol. 23, No. 2, pp. 16/1 - 4, August 2021.

Simulation study of different sensing directions in OPM and SQUID MEG

Urban Marhl[a,b], Tilmann Sander[c], and Vojko Jazbinšek[a]
[a]*Institute of Mathematics, Physics and Mechanics, Ljubljana, Slovenia*
[b]*Faculty of Natural Sciences and Mathematics, University of Maribor, Maribor, Slovenia*
[c]*Physikalisch-Technische Bundesanstalt, Berlin, Germany*

Correspondence: Urban Marhl, Institute of Mathematics, Physics and Mechanics,
Jadranska 19, SI-1000 Ljubljana, Slovenia
Email: urban.marhl@imfm.si Website: *https://urbanmarhl.com/* Phone: +386 147 66632

Abstract. Magnetoencephalography (MEG) measures magnetic fields in the vicinity of the subject's head. Due to the nature of the magnetic field, it is not the same when measured in different directions. This raises the question, in which direction to place the sensors to measure the largest possible signals. Now that optically pumped magnetometers (OPMs) are being used in MEG, this question is even more relevant since they can be placed arbitrarily on the subject's head. In this work we made a numerical simulation to check how the noise of spontaneous brain activity affects signal-to-noise ratio of different SQUID MEG sensor configurations and different components of OPM MEG system.

Keywords: magnetoencephalography; optically pumped magnetometer; superconducting quantum interference device; magnetic field map; equivalent current dipole

1. Introduction

Magnetoencephalography (MEG) is a neuroimaging method which maps magnetic fields in the vicinity of the head (Hämäläinen et al., 1993). In recent years MEG has had a lot of success, new sensors are being used, i.e., optically pumped magnetometers (OPMs). OPMs have many advantages over the standard SQUIDs, the main being that they do not require cooling with cryogenics for their operation (Kim et al., 2014). Therefore, sensors can be placed directly on subject's head. In recent simulation studies it was shown (Boto et al., 2016; Iivanainen et al., 2017) that the reduction of distance between sensors and head increases the signal-to-noise (SNR) ratio and spatial resolution.

Currently, most of the commercial OPM sensors can measure simultaneously different vector components of the magnetic field. Different components can also be measured by SQUID systems, where magnetometers are commonly combined into different types of gradiometers. In this work, we performed a numerical simulation, where we calculated magnetic fields of sources inside the brain on different sensor types and sensing components for both SQUID and OPM MEG systems. To the calculated fields, we added noise, which had origins inside the subject's head. We checked how this generated noise affects the calculated SNR.

2. Methods

Several sensor layouts for the SQUID and OPM MEG system were generated. The latter was constructed for each subject individually. In this study we used the MRI data of 9 subjects. To construct the OPM sensor layout, we extracted outer head surface points from the MRI using the Freesurfer software (Fischl, 2012). The sensors were placed reasonably all over the head, with a distance of approximately 2 cm between them. Therefore, the maximal number (around 100) of sensors that can be placed on a subject's head depends on the head size. When calculating the magnetic field, we assumed that each of the sensors can measure 3 orthogonal components. One component is radial (OPM RAD) and the other two are tangential to the heads outer surface. One tangential component is parallel to the transverse plane, i.e., along the lines of latitude (OPM TAN-LAT) and the other is perpendicular to the other two components, i.e., along the lines of longitude (OPM TAN-LON). For one subject the sensor

layout is presented in Fig. 1b). The base layout of the SQUID MEG system was taken from the Yokogawa system, which consists of 125 axial first-order gradiometers (Masahiro et al., 2004). The distance between two radial magnetometers that forms one axial gradiometer is 5 cm. We denote this type of sensors as SQUID RAD GRAD, and we used positions of magnetometers closer to the head to define layouts for 5 other types of sensors:

- SQUID TAN-LAT GRAD – planar gradiometer consists of two radial magnetometers separated by 1 cm along the lines of latitude,
- SQUID TAN-LON GRAD – planar gradiometer consists of two radial magnetometers separated by 1 cm along the lines of longitude,
- SQUID RAD MAG – radial magnetometer,
- SQUID TAN-LAT MAG – tangential magnetometer sensing along the lines of latitude,
- SQUID TAN-LON MAG – tangential magnetometer sensing along the lines of longitude.

The SQUID RAD MAG layout is shown on Fig. 1a). To position the subject head inside the SQUID-MEG system we used the co-registration results from real measurements with that subject.

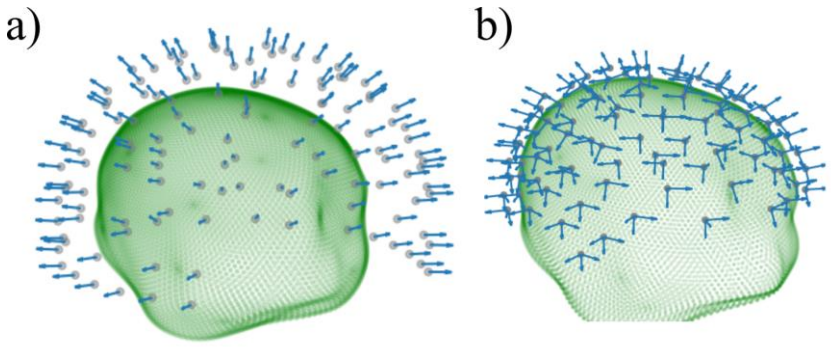

1. *Both (SQUID and OPM) MEG systems with headshape points of one subject. a) SQUID MEG systems consisting of 125 radial magnetometers (SQUID RAD MAG); b) OPM MEG system consisting of around 100 magnetometers, where each sensor has 3 sensing components.*

For all the sensor layouts listed above we calculated magnetic fields of sources inside the subject's head. For the forward model we used a simplified formula of sources inside a homogeneous spherical volume conductor (Sarvas, 1987). The center of the spherical volume conductor was at the center of the subject's brain, which we reconstructed from the MRI image. We performed 2 simulations of different sources. For the first simulation we identified for each subject the regions of auditory cortex on both hemispheres using software package Freesurfer and the Destrieux Atlas (Destrieux et al., 2010; Fischl, 2012). We placed two equivalent current dipoles (ECDs), one in the center of the left auditory cortex and the other in the center of the right auditory cortex. The dipole strength was 100 nAm. The direction was determined randomly for 1000 samples. For the second simulation we determined the locations and directions of 2 ECDs each in one hemisphere randomly on the cortical mantle also for 1000 samples. Note that in both simulations the vectors of directions were orthogonal to the vector, which points from the center of the spherical volume conductor to the dipole location.

For both simulations we added noise, which originates inside the head. The noise for one sample was generated with 100 randomly chosen dipoles on the cortical mantle with random locations. The strength of each "noisy" dipole was determined as:

$$p_{\text{noise}} = p\xi, \tag{1}$$

where ξ represent the Gaussian noise with 0 mean and standard deviation of 1. In the simulations we changed the value of p to obtain different noise levels.

To evaluate how internal noise affects the noise level of different SQUID and OPM MEG system layouts, we calculated the values of signal to noise ratio SNR (Ilmoniemi & Sarvas, 2019):

$$\text{SNR} = 20\log_{10}\left(\frac{\text{RMS}_{\text{signal}}}{\text{RMS}_{\text{noise}}}\right), \tag{2}$$

where $\text{RMS}_{\text{noise}}$ is the root mean square of generated noise and $\text{RMS}_{\text{signal}}$ the root mean square of data where we simulated "expected" sources with the added noise. Both values were averaged over all samples (1000 times).

3. Results

The magnetic field maps of simulation 1 are shown for one subject on Fig 2., where we can see the values of magnetic field maps of all the different MEG layouts for both SQUID and OPM MEG systems. The shape and strength of the magnetic field varies greatly for individual layouts.

In Table 1 we presented the values of SNR for both simulations. For each simulation case (1 and 2) we used 3 different noise strengths (low, medium, high).

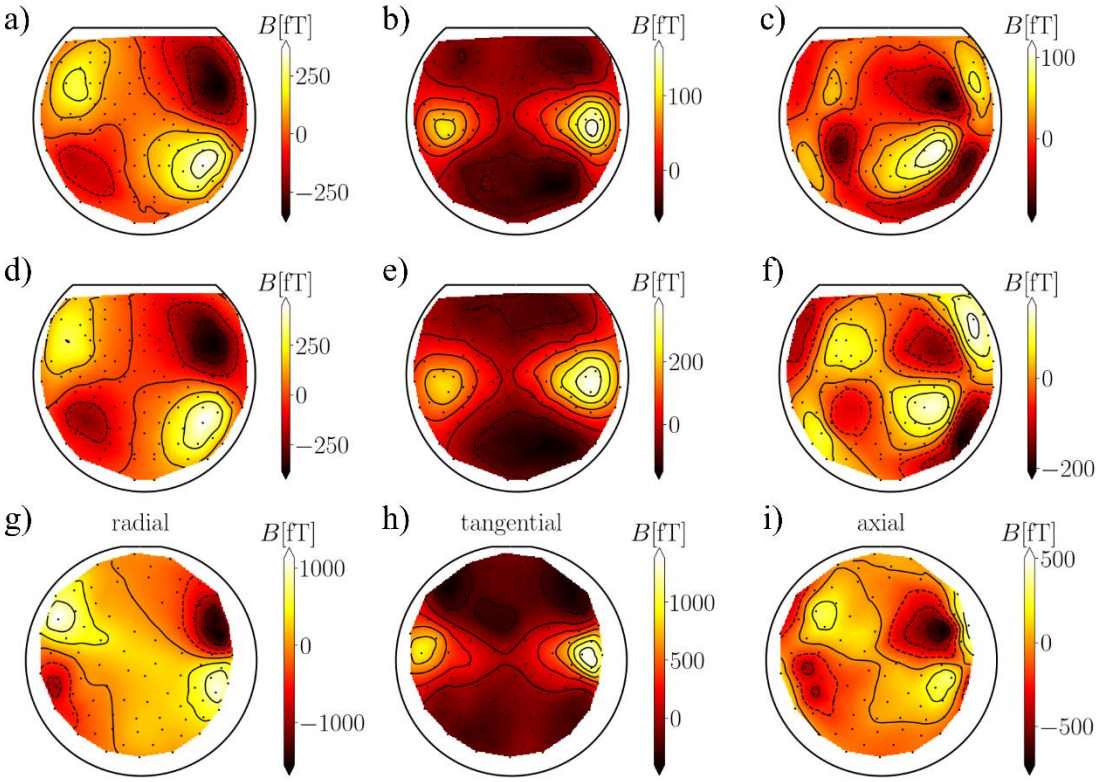

2. *Magnetic field maps for the SQUID and OPM-MEG layouts: a)* SQUID RAD GRAD, *b) SQUID TAN-LAT GRAD, c) SQUID TAN-LON GRAD, d) SQUID RAD MAG, e) SQUID TAN-LAT MAG and f)* SQUID TAN-LON MAG, *g)* OPM RAD, *h)* OPM TAN-LAT *and i)* OPM TAN-LON.

1. *Calculated and averaged values of SNR for all 9 subjects with calculated standard deviation for simulations 1 and 2 for different noise levels (strength of each noisy dipole). The values are shown for all SQUID-MEG sensor layouts and for different components of OPM-MEG system.*

Simulation	1	1	1	2	2	2
Noise strength (p [nAm]*)*	1	5	10	1	5	10
System			*SNR* [dB]			
SQUID RAD GRAD	19.46±1.00	6.52±0.78	2.76±0.45	24.02±0.18	10.50±0.14	5.52±0.17
SQUID TAN-LAT GRAD	19.89±1.32	6.91±1.08	2.97±0.61	24.00±0.40	10.36±0.33	5.45±0.28
SQUID TAN-LON GRAD	18.84±1.17	6.07±0.92	2.50±0.50	24.33±0.26	10.61±0.14	5.59±0.21
SQUID RAD MAG	18.18±1.48	5.57±1.10	2.23±0.61	22.49±0.98	9.01±0.87	4.40±0.62
SQUID TAN-LAT MAG	18.86±1.50	6.12±1.11	2.50±0.63	22.25±0.93	8.77±0.96	4.22±0.63
SQUID TAN-LON MAG	18.06±1.24	5.50±0.90	2.20±0.48	22.79±1.02	9.34±0.86	4.70±0.69
OPM RAD	19.92±0.82	6.89±0.64	2.96±0.42	24.24±0.17	10.56±0.13	5.65±0.11
OPM TAN-LAT	20.64±0.83	7.50±0.70	3.36±0.46	24.09±0.23	10.43±0.14	5.56±0.13
OPM TAN-LON	19.94±0.94	6.90±0.72	2.96±0.49	24.51±0.14	10.77±0.18	5.81±0.12
OPM - all combined	20.08±0.83	7.02±0.66	3.05±0.43	24.27±0.17	10.58±0.13	5.67±0.10

4. Discussion

Different components of the magnetic field at the same measuring site are very different, which can be seen clearly on Fig. 2 where we present magnetic field maps of different sensor configurations of the SQUID-MEG system and different measuring components of the OPM-MEG system. The OPM-MEG system has significantly higher field strengths than SQUID-MEG, which is the result of the proximity of OPM sensors to the subject's head.

When comparing the values in Table 1, SQUID Gradiometers outperform SQUID magnetometers in both simulations (1 and 2) for all noise strengths. OPM magnetometers outperform both SQUID magnetometer and gradiometer layouts. Note that these conclusions hold only when we compare the sensors which measure the same component. With increasing strength of the "noisy" dipoles, the SNR of all systems significantly drops. In simulation 1 these values fall lower than in simulation 2.

In simulation 1, the best results (highest SNR) are obtained with the tangential components along the lines of latitude (TAN-LAT) and the worst with the tangential components along the lines of longitude (TAN-LON). Results in simulation 2 differ, the best results (highest SNR) are obtained with the TAN-LON components and the worst with the TAN-LAT. This effect can be the result of the simplified forward model, for future work this should be tested with a more complex forward model (BEM). Also, it would be wise to check, if the increased SNR of the OPMs increases the goodness of fit of the fitted dipoles. In our work, we considered only the noise that is the result of spontaneous activity within the subject, if we would also consider the ambient noise, we expect that the OPM-MEG system due to the larger amplitude of the simulated data would have a significantly higher SNR than the SQUID-MEG system.

5. Conclusion

We simulated magnetic fields for sources within the subject's brain with added noise which represent spontaneous neural activity. First, we did a simulation of the sources within the auditory cortex and then the sources were chosen in random regions on the cortical mantle. Magnetic fields were calculated for different configurations of the SQUID-MEG system and for three different components of the OPM-MEG system. As expected, the amplitude of magnetic fields for the OPM-MEG system are much higher than for different SQUID-MEG sensor layouts. The values of SNR for OPM sensors are on average higher, than corresponding SNR for the SQUID magnetometers/gradiometers configurations. From the results we can conclude that the noise, which represents spontaneous brain activity, has slightly lower impact on the OPM-MEG system than on the SQUID-MEG systems.

Acknowledgments

Support from Slovenian Research Agency project ID P2-0348 and by DAAD project ID 57402032 is acknowledged.

References

Boto, E., Bowtell, R., Krüger, P., Fromhold, T. M., Morris, P. G., Meyer, S. S., Barnes, G. R., & Brookes, M. J. (2016). On the Potential of a New Generation of Magnetometers for MEG: A Beamformer Simulation Study. *PLOS ONE*, *11*(8), e0157655. https://doi.org/10.1371/journal.pone.0157655

Destrieux, C., Fischl, B., Dale, A., & Halgren, E. (2010). Automatic parcellation of human cortical gyri and sulci using standard anatomical nomenclature. *NeuroImage*, *53*(1), 1–15. https://doi.org/10.1016/j.neuroimage.2010.06.010

Fischl, B. (2012). FreeSurfer. *NeuroImage*, *62*(2), 774–781. https://doi.org/10.1016/j.neuroimage.2012.01.021

Hämäläinen, M., Hari, R., Ilmoniemi, R. J., Knuutila, J., & Lounasmaa, O. V. (1993). Magnetoencephalography—Theory, instrumentation, and applications to noninvasive studies of the working human brain. *Reviews of Modern Physics*, *65*(2), 413–497. https://doi.org/10.1103/RevModPhys.65.413

Iivanainen, J., Stenroos, M., & Parkkonen, L. (2017). Measuring MEG closer to the brain: Performance of on-scalp sensor arrays. *NeuroImage*, *147*, 542–553. https://doi.org/10.1016/j.neuroimage.2016.12.048

Ilmoniemi, R., & Sarvas, J. (2019). *Brain signals: Physics and mathematics of MEG and EEG*. The MIT Press.

Kim, K., Begus, S., Xia, H., Lee, S.-K., Jazbinsek, V., Trontelj, Z., & Romalis, M. V. (2014). Multi-channel atomic magnetometer for magnetoencephalography: A configuration study. *NeuroImage*, *89*, 143–151. https://doi.org/10.1016/j.neuroimage.2013.10.040

Masahiro, S., Hiroaki, T., Kunio, K., & Yasuhiro, H. (2004). MEGvision magnetoencephalograph system and its applications. *Yokogawa Technical Report English Edition*, *38*, 23–27.

Sarvas, J. (1987). Basic mathematical and electromagnetic concepts of the biomagnetic inverse problem. *Physics in Medicine and Biology*, *32*(1), 11–22. https://doi.org/10.1088/0031-9155/32/1/004